squalene aldehyde[3] by using the same procedure as above (14 mg, 29%, R_f = 0.24, 20% EA/H): IR (neat) 3343.1, 1666.4 cm^{-1}; ^1H NMR ($CDCl_3$) δ 1.49 (quintet, J = 6.6 Hz, 2 H, C-3 CH_2), 1.60 (br s, 15 H, C-24, C-25, C-26, C-27, C-28 CH_3), 1.68 (s, 3 H, C-23 CH_3), 2.00 (br m, 20 H, C-2 CH_2 and C=CCH_2), 3.64 (t, J = 6.3 Hz, 2 H, CH_2OH), 5.12 (br m, 5 H, C=CH); ^{13}C NMR ($CDCl_3$) δ 15.82, 16.02, 17.66 (C-24, C-25, C-26, C-27, C-28), 24.00 (C-23), 25.68 (C-3), 26.62, 26.65, 26.77 (C-7, C-16, C-20), 28.26 (C-11, C-12), 32.32 (C-2), 39.32, 39.73 (C-4, C-8, C-15, C-19), 62.98 (C-1), 124.27, 124.39, 124.55 (C-6, C-10, C-13, C-17), 131.23 (C-22), 134.69, 134.88, 135.03, 135.10 (C-5, C-9, C-14, C-18). Anal. Calcd: C, 83.83; H, 12.08. Found: C, 83.94; H, 12.27.

IC_{50} Determinations for Inhibition of SE and OSC. Test tubes containing either squalene epoxidase or oxidosqualene cyclase enzyme solutions[3] (240 μL each) were warmed to 37 °C. After 10 min, squalene analogues were added (1 μL in 2-propanol) to give final inhibitor concentrations of 0, 4, 20, 40, 200, and 400 μM. After an additional 10 min, [^{14}C]squalene (2 μL in 2-propanol, ca. 20000 dpm, 33 μM)[3] was added to each enzyme solution. Incubation was continued for another 50 min and then stopped by the addition of 10% KOH/methanol (240 μL). After 1 h at 37 °C, each mixture was extracted with CH_2Cl_2 (1 mL each); the resulting organic extracts were dried ($MgSO_4$) and redissolved in a small amount of CH_2Cl_2 (100 μL), and the triterpene components were separated by thin-layer chromatography. Radiochemical analysis, using either linear analysis or scintillation counting, showed conversion of squalene to either 2,3-epoxysqualene (for the epoxidase assays), or a mixture of lanosterol and 2,3-epoxysqualene (for the cyclase assays). Inhibitor-free assays showed approximately 30% conversion to product, and radiochemical recoveries of 80%–90% were routinely achieved.

Acknowledgment. We thank Dr. Gregory M. Anstead for the preparation of trisnorsqualene methyl carbinol, and we acknowledge the Center of Biotechnology and the New York State Science and Technology Program and the Kirin Brewery Co., Ltd. for financial support.

All Atom Molecular Mechanics Simulations on Covalent Complexes of Anthramycin and Neothramycin with Deoxydecanucleotides

Shashidhar N. Rao*,† and William A. Remers‡

Searle Research and Development, Division of G. D. Searle and Company, 4901 Searle Parkway, Skokie, Illinois 60077, and College of Pharmacy, University of Arizona, Tucson, Arizona 85721. *Received July 14, 1989*

We present molecular mechanics simulations on covalent complexes between d[$(GC)_5$]$_2$, d(G_{10})·d(C_{10}), d-(GCGCGAGCGC)·d(GCGCTCGCGC), d(GCGCGTGCGC)·d(GCGCACGCGC), d(G_5AG_4)·d(C_4TC_5), and d-(G_5TG_4)·d(C_4AC_5) on one hand and potent antitumor antibiotics anthramycin and neothramycin A on the other, using the all atom force field in the framework of the program AMBER(UCSF). The energy-refined models of both the sets of complexes show minimal distortions for the nucleotides, consistent with the results of 2D NMR studies on these complexes. The drugs have 3′-orientation in the minor groove, consistent with the previously reported investigations employing the united atom force field and with the experimental observations. Both anthramycin and neothramycin are calculated to bind preferentially to the puGpu sequences over pyGpy. This is in qualitative agreement with experimental studies for anthramycin, while for neothramycin A, this result is in apparent disagreement with experimental observations which have reported preferential binding of neothramycin A to poly(dG-dC)·poly(dG-dC) over poly(dG)·poly(dC). While the present study brings out the usefulness of the simple molecular mechanics approach (using an all atom force field) in rationalizing substantial experimental observations, it also emphasizes the need for further investigations on solvent and dynamics effects in understanding the sequence specificity of drug–DNA binding.

Pyrrolo[1,4]benzodiazepines (PBDs) (Figure 1) are potent antitumor antibiotics derived from various streptomyces species[1,2] and act by binding in the minor groove of DNA and alkylating it on the 2-amino group of a guanine residue.[3–8] This groove binding is facilitated by a twist in the PBD structure, fixed by the chiral center at C11a, that gives it a precise fit to right-handed B-DNA.[9,10] As shown in Scheme I, the DNA alkylation occurs at C11 of the PBD. This carbon occurs in a variety of substitution patterns: carbinolamine, carbinolamine ether, or imine, but all of them are potential alkylating groups. The precise mechanism or mechanisms of alkylation are not defined at this time; however, it is possible that initial noncovalent binding, stabilize by a network of hydrogen bonds and van der Waals interactions, positions the molecule for subsequent covalent bond formation. Computer modeling indicates that this is a reasonable scenario.[11] Detailed structures of the covalent complexes have been provided by NMR studies,[7,12] some of which were made in conjunction with computer modeling.[13,14]

The sequence specificity for binding of PBDs to double helical DNA is thought to be important in their antitumor activity.[15,16] It also is fundamental to their potential use as DNA probes. An early study on the binding of an-

Scheme I. Alkylation of DNA (2-Amino Group of G) at C11 of a Typical PBD

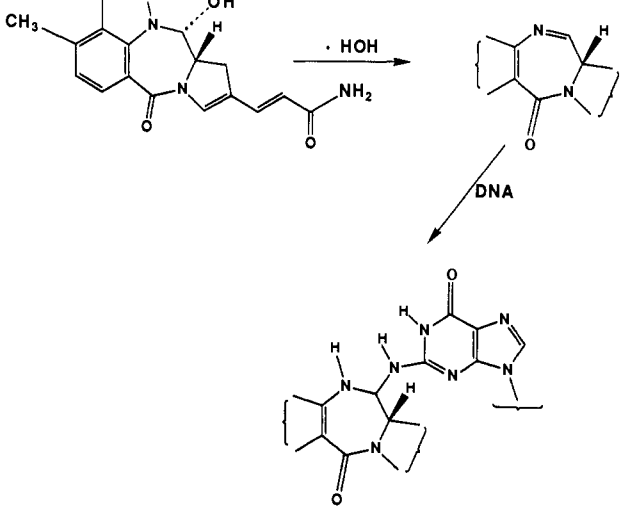

*To whom correspondence should be addressed.
†G. D. Searle and Co.
‡University of Arizona.

(1) Hurley, L. H. *J. Antibiotics* 1977, *30*, 349.

0022-2623/90/1833-1701$02.50/0

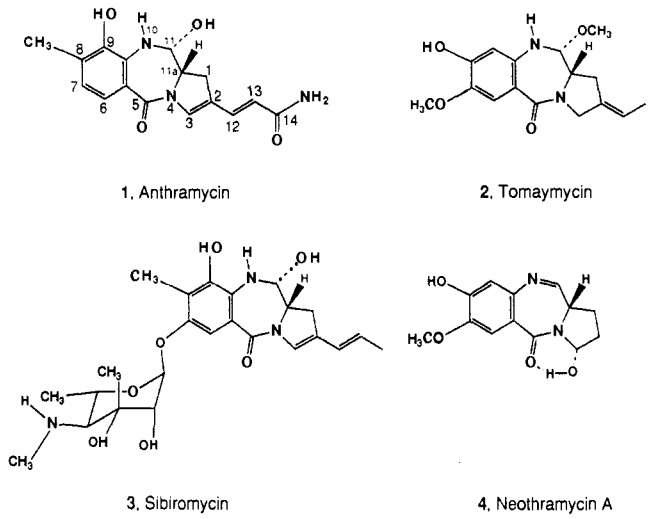

Figure 1. Structures of some pyrrolo[1,4]benzodiazepines.

thramycin (1) showed that it reacted as strongly with poly(dG)·poly(dC) as it did with calf thymus DNA, but it did not react with polynucleotides lacking dG residues.[17] Subsequent investigations based on sequence determination by footprinting with methidium of DNA-bound anthramycin revealed a strong preference for binding to puGpu sequences, with pyGpy sequences being the least preferred.[15] Sequences containing puGpy and pyGpu showed intermediate binding preferences. Parallel results were found with tomaymycin (2) and sibiromycin (3).[15] In marked contrast to these results was the report that neothramycin (4) bound strongly to poly(dG·dC)·poly(dG·dC), but it had little or no binding to poly(dG)·poly(dC).[18]

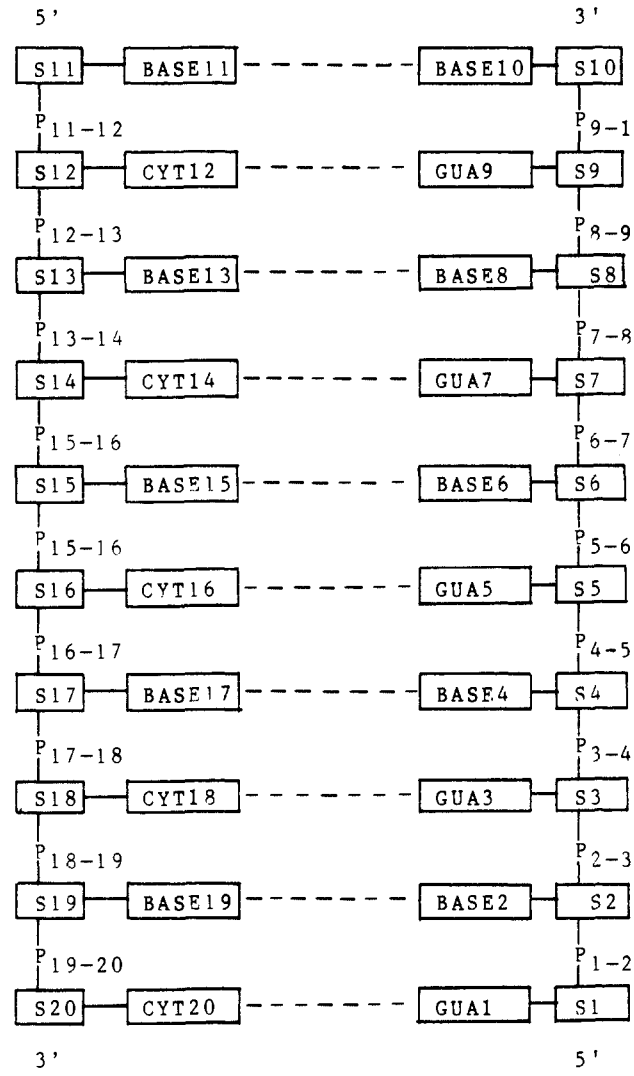

Figure 2. Schematic for decanucleotide duplexes. S stands for sugar.

Sequence studies were not performed on neothramycin–DNA covalent complexes.

Computer modeling of the binding of PBDs to polynucleotide duplexes has had some success in predicting the preferred conformations of the resulting complexes. For both tomaymycin[13] and anthramycin,[11,14,19] calculations that predicted the preferred direction for the drug to lie in the minor groove and the configuration of the alkylating carbon atom were completely consistent with the results of the 2D NMR and fluorescence emission studies.[13] A recent study on the sequence specificity of DNA binding for PBDs gave results that were consistent with footprinting experiments,[20] although there were inconsistencies with the detailed structures of the adducts as shown by 2D NMR studies.[13]

On the basis of results described obtainable so far in the literature, two main goals were set for the present investigation. One of them involved the use of molecular mechanics to explore the problem of neothramycin sequence specificity. It seemed important to learn, if possible, why this agent has a selectivity for poly(dG·dC) which is opposite (puGpu) to that exhibited by other PBDs. The second objective was to reexamine the usefulness of the

(2) Remers, W. A. *The Chemistry of Antitumor Antibiotics*; Wiley-Interscience: New York, 1988; Vol. 2, pp 28–92.
(3) Kohn, K. W.; Spears, C. L. *J. Mol. Biol.* **1970**, *51*, 551.
(4) Glaubiger, D.; Kohn, K. W.; Charney, E. *Biochim. Biophys. Acta* **1974**, *361*, 303.
(5) Hurley, L. H.; Allen, C.; Feola, J.; Lubawy, W. C. *Cancer Res.* **1979**, *39*, 3134.
(6) Hurley, L. H.; Petrusek, R. *Nature* **1979**, *282*, 529.
(7) Graves, D. E.; Pattaroni, C.; Krishnan, B. S.; Ostrander, J. M.; Hurley, L. H.; Krugh, T. R. *J. Biol. Chem.* **1984**, *259*, 8202.
(8) Barkley, M. D.; Cheatham, S.; Thurston, D. E.; Hurley, L. H. *Biochemistry* **1986**, *25*, 3021.
(9) Mostad, A.; Romming, C.; Storm, B. *Acta Chem. Scand.* **1978**, *32*, 39.
(10) Arora, S. K. *Acta Crystallogr.* **1979**, *B35*, 2945.
(11) Remers, W. A.; Mabilia, M.; Hopfinger, A. J. *J. Med. Chem.* **1986**, *29*, 2492.
(12) Graves, D. E.; Stone, M. P.; Krugh, T. R. *Biochemistry* **1985**, *24*, 7573.
(13) Cheatham, S.; Kook, A.; Hurley, L. H.; Barkley, M. D.; Remers, W. A. *J. Med. Chem.* **1988**, *31*, 583.
(14) Boyd, F. L.; Cheatham, S.; Remers, W. A.; Hill, G. C.; Hurley, L. H. *J. Am. Chem. Soc.*, in press.
(15) Hertzberg, R. P.; Hecht, S. M.; Reynolds, V. L.; Molineux, I. J.; Hurley, L. H. *Biochemistry* **1986**, *25*, 1249.
(16) Hurley, L. H.; Reck, T.; Thurston, D. E.; Langley, D. R.; Holden, K. G.; Hertzberg, R. P.; Hoover, J. R. E.; Gallagher, G., Jr.; Faucette, L. F.; Mong, S.-M.; Johnson, R. K. *Chem. Res. Toxicol.* **1988**, *1*, 258–268.
(17) Kohn, K. W.; Glaubiger, D.; Spears, C. L. *Biochim. Biophys. Acta* **1974**, *361*, 288.
(18) Maruyama, I. N.; Tanaka, N.; Kondo, S.; Umezawa, H. *J. Antibiot.* **1979**, *32*, 928.
(19) Rao, S. N.; Singh, U. C.; Kollman, P. A. *J. Med. Chem.* **1986**, *29*, 2484.
(20) Zakrzewska, K.; Pullman, B. *J. Biomol. Struct. Dyn.* **1986**, *4*, 127.

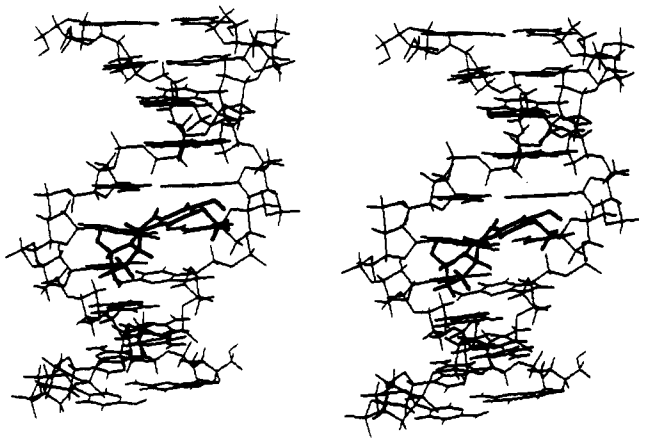

Figure 3. Stereo pair of energy-minimized NEO-GC10 (*S*,3′).

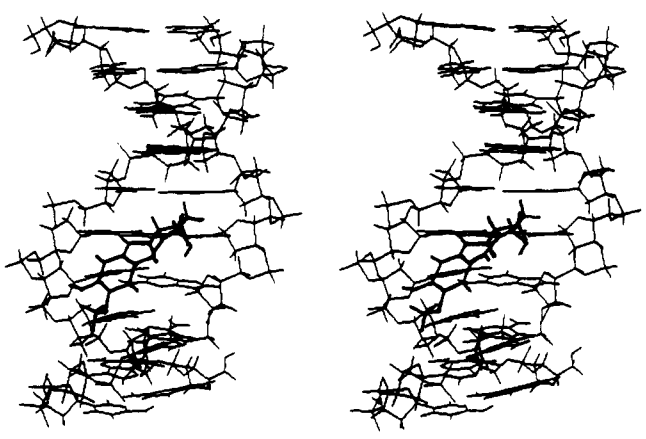

Figure 4. Stereo pair of energy-minimized NEO-GC10 (*S*,5′).

AMBER force field[21] in predicting sequence specificity of anthramycin, with the all atom force field[22] for the decanucleotides, rather than the previously used united atom force field.[23]

Results and Discussions

Neothramycin. This agent occurs naturally as a mixture of neothramycin A and neothramycin B (epimeric at C2).[24] In the previous study, the former was chosen and the AMBER united atom force field was used. The configuration at C11 was not specified, but it became *S* after energy minimization.[11] For the present study, neothramycin A was used and the covalent drug–polynucleotide complex was modeled with both configurations at C11 to ensure that the previous result was correct. Both directions in the minor groove were modeled and the all atom force field was used for both neothramycin and the polynucleotides. We have not previously encountered substantial differences in the results between all atom and united atom models involving PBDs, but the preferred orientation for intercalative ethidium binding to d-$(GCGCGC)_2$ was predicted correctly only by the all atom force field.[25]

Energies for minimized covalent complexes between neothramycin A and the decanucleotides are listed in Table I. There are four different conformations for NEO-GC10 reflecting the two orientations and two configurations at C11. The preferred conformation for NEO-GC10 is clearly the one with *S* configuration at C11 and the benzene ring of neothramycin pointing in the 3′-direction (Figure 3). Most of its advantage comes from increased intermolecular interactions, rather than decreased helix distortion. The sources of this increased binding energy can be found in Table II, which lists the interactions between neothramycin and individual residues in the polynucleotide (see Figure 2). The complex with 3′,*S* geometry has at least twice as many significant (−3.0 kcal/mol) interactions as any of the other three. Hydrogen bonding (Table III) is not an important contributor to intermolecular attraction. Only the 3′,*R* geometry has an

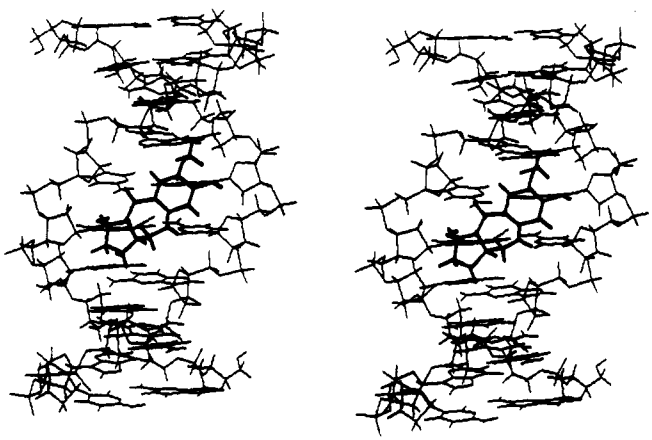

Figure 5. Stereo pair of energy-minimized NEO-GC10 (*R*,3′).

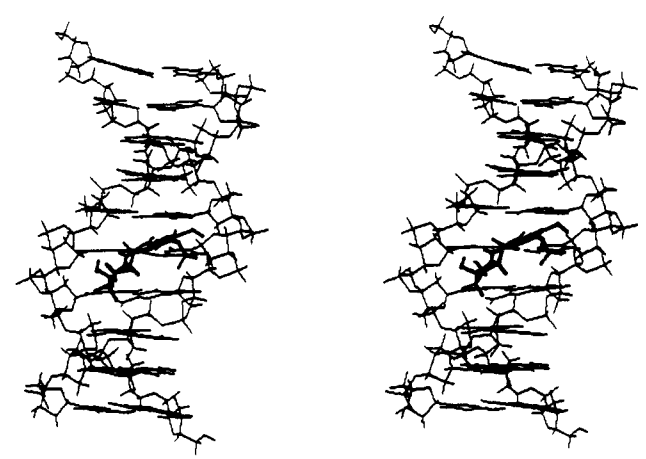

Figure 6. Stereo pair of energy-minimized NEO-GC10T6 (*S*,3′).

intermolecular bond for NEO-GC10, although most of the complexes in this table have intramolecular hydrogen bond between HO2 and O4 (see Figure 1).

For NEO-G10C10, there are two preferred conformations, both with the benzene ring of the drug pointing in the 3′-direction. One has *S* configuration (Figure 4) and the other has *R* configuration (Figure 5). Their superior net binding energies derive more from low helix distortion energy than from increased intermolecular binding (Table I). The number of good interactions with individual residues is nearly the same for all conformations except 5′,*R*, which has only one (Table II). This complex is the only one in which the O2H forms a hydrogen bond with the polynucleotide (Table III). A comparison of the net binding energies for NEO-GC10 and NEO-G10C10 ap-

(21) Singh, U. C.; Weiner, P. K.; Caldwell, J. W.; Kollman, P. A. AMBER(UCSF) version 3.0; Department of Pharmaceutical Chemistry, University of California, San Francisco, CA 94143, 1986.
(22) Weiner, S. J.; Kollman, P. A.; Nguyen, D.; Case, D. *J. Comput. Chem.* **1986**, *7*, 230–252.
(23) Weiner, S. J.; Kollman, P. A.; Case, D.; Singh, U. C.; Ghio, C.; Alagona, J.; Profeta, S., Jr.; Weiner, P. K. *J. Am. Chem. Soc.* **1984**, *106*, 765–785.
(24) Miyamoto, M.; Kondo, S.; Naganawa, H.; Maeda, K.; Umezawa, H. *J. Antibiotics* **1977**, *30*, 340.
(25) Lybrand, T. P.; Kollman, P. A. *Biopolymers* **1985**, *24*, 1863.

Table I. Total, Intermolecular, Intramolecular, and Net Binding Energies (in kcal/mol) in the Covalent Complexes between Pyrrolo[1,4]benzodiazepines and Decanucleotides

			intermolecular			intramolecular					
complex	orientation	total	elec[a]	vdw	$E_{d\text{-}h}$	Hel1[b]	Hel2	E_{dis}[c]	E_d[d]	E_{ddis}	E_{netb}
NEO-GC10	*S*,3′	-829.9	-18.6	-24.9	-43.5	-819.9	-800.7	19.2	14.2	1.8	-22.5
	S,5′	-817.3	-11.9	-19.0	-30.9	-819.9	-802.2	17.1	15.9	3.5	-9.7
	R,3′	-810.5	-18.3	16.7	-35.0	-819.9	-793.0	26.9	17.4	5.0	-3.1
	R,5′	-813.0	-8.7	-22.3	31.0	-819.9	-797.6	22.3	15.6	3.2	-5.5
NEO-G10C10	*S*,3′	-813.3	-16.2	-22.6	-38.8	-802.4	-787.0	15.4	12.7	0.3	-23.1
	S,5′	804.2	-10.9	-27.5	-38.4	-802.4	-778.3	24.1	12.5	0.1	-14.2
	R,3′	-811.3	-15.8	-24.0	-39.8	-802.4	-785.1	17.3	13.5	1.1	-21.4
	R,5′	-795.7	-12.8	-24.0	-36.8	-802.4	-772.5	29.9	13.6	1.2	-5.7
NEO-GC10A6	*S*,3′	-773.8	-14.9	-22.8	-37.7	-771.3	-751.4	-19.9	15.3	0.9	-16.9
NEO-GC10T6	*S*,3′	-772.6	-13.4	-21.2	-34.6	-772.6	-752.0	20.6	14.0	2.6	-11.4
ANT-GC10	*R*,3′	-823.1	-35.3	-29.5	-64.8	-814.4	-780.6	33.8	15.9	8.7	-22.3
	S,3′	-845.8	-36.7	-32.1	-68.8	-814.4	-794.1	20.3	15.9	8.7	-39.8
ANT-G10C10	*R*,3′	-801.3	-30.2	-30.3	-60.5	-790.4	-758.1	32.3	9.7	2.5	-25.7
	S,3′	-823.9	32.6	-33.1	-65.7	-790.4	-769.7	20.7	10.7	3.5	-41.5
ANT-GC10A6	*S*,3′	-818.0	-35.7	-32.2	-67.9	-787.3	-766.4	20.9	15.5	8.3	-38.7
ANT-GC10T6	*S*,3′	-819.7	-36.8	-32.0	-68.8	-788.3	-767.8	20.5	15.8	8.6	-39.7
ANT-G10C10A6	*S*,3′	-799.7	-29.1	-33.7	-62.8	-768.3	-748.4	19.9	10.5	3.2	-39.6
ANT-G10C10T6	*S*,3′	-798.5	-30.0	-33.1	-63.1	-767.5	-747.1	20.4	10.7	3.5	-39.3

[a] In the AMBER force field, the electrostatic component of hydrogen bonds is evaluated as a normal Coulombic interaction with distance-dependent dielectric constant and is included with the electrostatic energy term. The steric component of hydrogen-bonding interaction is evaluated through a 10-12 van der Waals term, which accounts for only a small portion of the total hydrogen-bonding interactions (±1.5 kcal/mol). [b] The energies of isolated helices (Hel1) were determined by starting with the minimized drug-DNA complexes, removing the drug, replacing the hydrogen on the 2-amino group of GUA5, and reminimizing the energy. The lowest value obtained for a particular helix is used in the table for comparison with all drug-DNA complexes containing this helix. [c] The helix distortion energy is the energy of the helix in a complex (Hel2) minus the energy of the isolated helix (Hel1). [d] Drug distortion energy is the energy of the drug in a complex minus the energy of the minimized isolated drug. The energies for isolated neothramycin A and anthramycin are respectively 12.4 and 7.2 kcal/mol. [e] The net binding energy is the total intermolecular binding energy minus the combined helix and drug distortion energies.

Table II. Interaction Energies[a] (in kcal/mol) between Individual DNA Residues[b] and Pyrrolo[1,4]benzodiazepines

complex	orientation	GUA5	P1	S6	B6	GUA7	B15	CYT16	P2	B17	P3	S18	P4
NEO-GC10	*S*,3′	-5.1		-4.2	-5.8	-3.6		-3.5	-7.3				
	S,5′				-3.2			-3.8					
	R,3′							-5.6	-3.6				
	R,5′				-3.3		-3.9			-6.0			
NEO-G10C10	*S*,3′	-4.5			-5.1	-3.7		-3.4	-8.0				
	S,5′	-3.4						-3.2		-6.2		-5.0	
	R,3′	-5.0			-4.7	-4.4							
	R,5′							-3.2	-7.7				
NEO-GC10A6	*S*,3′	-5.6			-4.3	-3.5		-3.1	-4.8				
NEO-GC10T6	*S*,3′	-4.6	-3.3					-3.8			-3.1		
ANT-GC10	*R*,3′		-11.5					-13.4	-3.3	-4.5			
	S,3′	-4.2	-12.5		-6.4		-3.8	-10.5	-3.4				
ANT-G10C10	*R*,3′		-11.4					-6.6	-6.7	-3.4			
	S,3′	-4.8			-7.6			-3.6	-3.5	-3.2			-11.2
ANT-GC10A6	*S*,3′	-4.3	-12.5		-5.3		-3.7	-10.8	-3.1	-3.5			
ANT-GC10T6	*S*,3′	-4.3	-12.6		-5.7		-3.8	-10.5		-3.4			
ANT-G10C10A6	*S*,3′	-4.7			-4.7			-3.7	-3.4	-3.2			-11.1
ANT-G10C10T6	*S*,3′	-4.8			-4.5			-3.5	-3.4	-3.2			-11.1

[a] In addition to these interactions, the drug in NEO-G10C10 (R,5′) has an interaction of -4.3 kcal/mol with CYT4. [b] The groups represented by P1, P2, P3, P4, B6, B15, and B17 are respectively $P_{5\text{-}6}$, $P_{16\text{-}17}$, $P_{17\text{-}18}$, $P_{18\text{-}19}$, and bases numbered 6, 15, and 17, respectively (see Figure 2 for illustration).

pears to favor the latter, because it has two preferred conformations approximately equal in energy to the one preferred conformation of the former. The comparison leads to a prediction of binding selectivity for poly(dG)·poly(dC) which is consistent with the sequence specificity found for the other PBDs, but contrary to experimental evidence based on the binding of radiolabeled neothramycin to polynucleotides.

The complexes NEO-GC10A6 and NEO-GC10T6, in which the sixth base pair of GC10 was replaced by A-T and T-A, respectively, were modeled only in the 3′,*S* conformation, based on the strong preference for this conformation in NEO-GC10. Moderately strong binding for neothramycin was found for NEO-GC10A6 (Table I, Figure 6), but NEO-GC10T6 bound rather weakly. There were five drug-DNA interactions of greater than 3 kcal/mol in magnitude (Table II), but no intermolecular hydrogen bonds (Table III). The causes for their lower binding energies than those of the corresponding 3′*S* conformations for NEO-GC10 and for NEO-G10C10 are lower intermolecular binding and greater helix distortion, respectively (Table I).

The largest single source of helix distortions in NEO-DNA complexes is a weakening of Watson-Crick pairing between the guanine that bears the drug and the complementary cytosine. Energies of the -12.7 to -16.1 kcal/mol are obtained, in comparison with a normal value of around -21.5 kcal/mol. Other significant distortions are related to base-stacking energies (Table IV; supplementary material). Table V (supplementary material) lists the backbone dihedral angles and glycosidic torsions that differ by more than 30° from standard values for B-DNA. Only the P-O3′ torsion showed such differences. They were clustered in two areas of the oligonucleotide duplexes: from base 6 through base 9 in the strand bound covalently to the drug and from base 15 through base 19 in the com-

Table III. Hydrogen-Bonding Parameters Involving Pyrrolo[1,4]benzodiazepine-Polynucleotide Interactions[a]

complex	orientation	donor (X–H)	acceptor atom (Z)	length, Å	angle, deg
NEO-GC10	*R*,3′	N11–HN11(NEO)	O2(CYT16)	1.96	124.6
NEO-G10C10	*S*,5′	N11–HN11(NEO)	O2(CYT17)	1.94	144.0
	R,5′	O2–HO2(NEO)	O2(CYT17)	2.25	123.2
ANT-GC10	*R*,5′	O9–HO9(ANT)	O2(CYT16)	1.83	157.8
	R,5′	N11–HN11(ANT)	O2(CYT16)	1.86	139.6
	R,5′	N18–H181(ANT)	OB(P_{5-6})	2.00	159.4
	S,5′	O9–HO9(ANT)	O2(CYT16)	1.81	169.8
	S,5′	N18–H181(ANT)	OB(P_{5-6})	1.97	151.4
	S,5′	N11–HN11(ANT)	O2(CYT6)	2.16	122.7
ANT-G10C10	*S*,5′	N18–H181(ANT)	OA(P_{17-18})	1.97	147.1
	S,5′	N11–HN11(ANT)	N3(GUA6)	2.27	129.2
	S,5′	N2–HN2B(GUA6)	O9(ANT)	1.73	172.4
	R,5′	N2–HN2B(GUA6)	O9(ANT)	2.11	124.8
	R,5′	N18–H181(ANT)	OB(P_{5-6})	2.00	156.6
	R,5′	N11–HN11(ANT)	O2(CYT16)	1.95	130.2
	R,5′	O9–HO9(ANT)	O3′(P_{15-16})	2.80	129.7
ANT-GC10A6	*S*,5′	O9–HO9(ANT)	O2(CYT16)	1.81	172.3
	S,5′	N11–HN11(ANT)	N3(ADE6)	2.26	128.9
	S,5′	N18–H181(ANT)	OB(P_{5-6})	1.98	151.9
ANT-GC10T6	*S*,5′	O9–HO9(ANT)	O2(CYT16)	1.98	111.0
	S,5′	N11–HN11(ANT)	O2(THY6)	2.03	130.2
	S,5′	N18–H181(ANT)	OB(P_{5-6})	1.97	152.0
ANT-G10C10A6	*S*,5′	N18–H181(ANT)	OA(P_{17-18})	1.97	146.3
	S,5′	N11–HN11(ANT)	N3(ADE6)	2.27	126.4
ANT-G10C10T6	*S*,5′	N18–H181(ANT)	OA(P_{17-18})	1.97	146.7
	S,5′	N11–HN11(ANT)	O2(THY6)	2.08	125.4

[a] In a hydrogen bond X–H···Z, X and Z respectively represent the donor and the acceptor atoms. The hydrogen-bond length corresponds to the distance between H and Z, while the angle is X–H···Z.

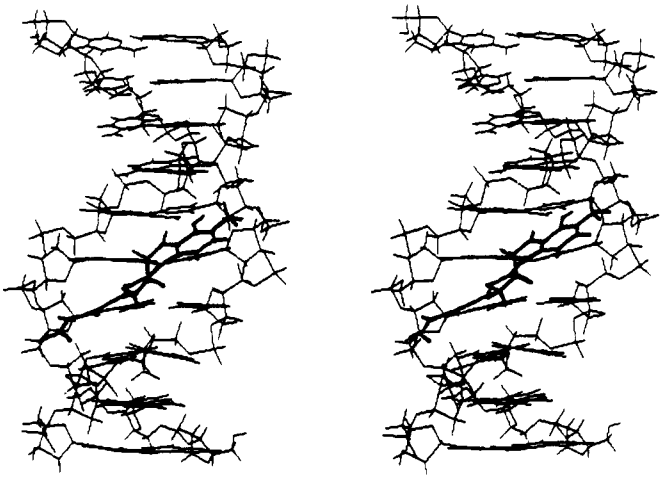

Figure 7. Stereo pair of energy-minimized ANT–GC10 (*S*,3′).

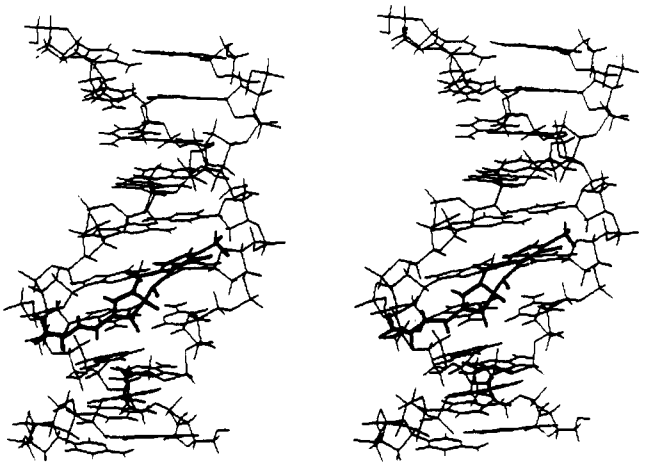

Figure 8. Stereo pair of energy-minimized ANT–GC10 (*R*,3′).

plementary strand (see Figure 2 for a schematic representation). The glycosidic torsions differeing from the standard values involved G1 in all the models and G11 in three of the four NEO–GC10 models. There were also a number of sugar puckers that differ from the standard C2′ endo in B-DNA containing G and C residues. Values of their phase angles (*W*) are listed in Table VI (supplementary material). Many of them have C1′ exo puckers (*W* = 108°–144°) and some have O1′ endo puckers (*W* = 72°–108°).

Anthramycin. As in NEO–DNA complexes, significant conformational changes are observed only around P–O3′ and glycosidic bonds (Table V, supplementary material) and in sugar puckers (Table VI, supplementary material) in ANT–DNA complexes, and hence are not discussed further. Figure 7 shows a stereo pair of the most stable anthramycin–GC10 complex, ANT–GC10 (*S*,3′). Unlike in the case of NEO–GC10, here the larger helix distortion in ANT–GC10 (*R*,3′) (Figure 8) is an important factor in such a preference (Table I). The larger helix distortion in ANT–GC10 (*R*,3′) is due to the loss of one of the three Watson–Crick hydrogen bonds between the covalently

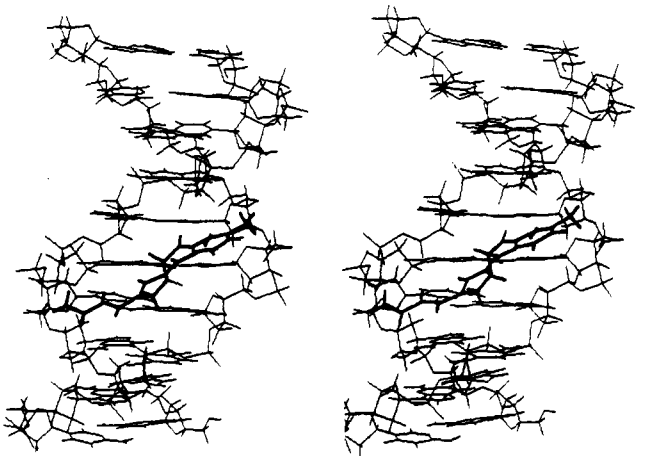

Figure 9. Stereo pair of energy-minimized ANT–G10C10 (*S*,3′).

linked guanine and its complementary cytosine. The net drug–helix interactions are favored in ANT–GC10 (*S*,3′) over ANT–GC10 (*R*,3′) by more than 17 kcal/mol. In ANT–GC10 complexes the amide side chain of anthra-

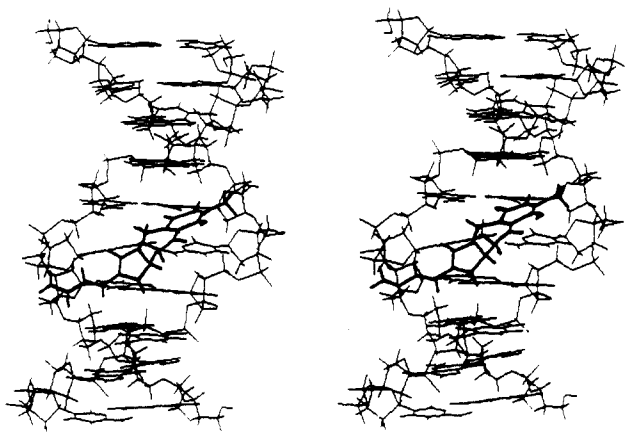

Figure 10. Stereo pair of energy-minimized ANT–G10C10 (*R*,3′).

mycin hydrogen bonds with P_{5-6} and the O9–HO9 hydroxyl hydrogen bonds with O2 of CYT16. Each of these H bonds leads to more than 10 kcal/mol of favorable interaction energy with the drug (Table II).

The G10C10–ANT complexes also prefer the *S* configuration at C11 and the 3′ direction of the benzene ring (Figure 9). ANT–G10C10 (*S*,3′) lacks the hydrogen bond between P_{5-6} and the amide side chain of the drug. Instead, the latter is hydrogen bonded with P_{18-19} on the complementary chain (Table III). In ANT–G10C10 (*R*,3′) the amide side chain hydrogen bonds with P_{5-6} and not P_{18-19} (Figure 10). The helix distortions are higher in ANT-G10C10 (*R*,3′) due to the loss of one of the Watson–Crick hydrogen-bonding interactions and the net binding is better in ANT-G10C10 (*S*,3′) by over 15 kcal/mol.

The net binding preference of anthramycin to G10C10 (*S*) by about 2.7 kcal/mol over GC10 (*S*) is qualitatively consistent with recent footprinting studies which show that the drug strongly prefers the puGpu sequences (GGG in this study) over the pyGpy sequences (CGC in this study). The calculated preference could be partly attributed to higher distortions of the drug in GC10 complexes.

The stereo pairs of the complexes containing A-T and T-A base pairs are available in the microfilm edition as supplementary material. The helix distortions in the four A-T-containing complexes are different only by an insignificant amount (1 kcal/mol). The net binding of the drug also shows no significant preference for one decanucleotide over the other (these energies differ at most by 1 kcal/mol).

Despite the very simplistic treatment of electrostatic and hydrogen-bonding effects in the AMBER force field and the lack of explicit counterion and solvent atmosphere, it is interesting that the most preferred binding sequence (puGpu) is calculated to have most favored binding energy with anthramycin. This correlation is stronger in the case of GC10 and G10C10 compared to the A- and T-containing decamers, and this could be probably attributed to dynamic effects not investigated in the present study. We also note that the carbonyl group on the five-membered ring of anthramycin is not hydrogen bonded with any of the nucleotide components in all the complexes. The role of such a group may be more evident in full simulations including waters and counterions.

Comparing the models obtained in this study for anthramycin–DNA complexes with the corresponding united atom models, we find that the two sets of models are structurally very similar. The minimum-energy structures correspond to the *S*,3′ configuration of the drug, consistent with the united atom models[19] and experimental observations.[12,14] In the light of this consistency and in the light of similar consistency obtained for other drug–DNA systems, the all atom approach is a reasonable one to start further simulations on ANT–DNA and NEO–DNA complexes which have explicit representations of solvent and counterions.

Table VII. Comparison of Energies (kcal/mol) for GC10 Derived from the Neothramycin–GC10 Complex and from Arnott's B-DNA Geometry (ref 29) (GC10_X)

	energy		
parameter	GC10	GC10_X	difference
h bond (10–12)	−3.2	−3.3	0.1
van der Waals	−232.6	−226.0	−6.6
electrostatic	−862.9	−843.1	−19.8
bond length	7.9	7.4	0.5
bond angle	81.5	73.3	8.2
dihedral	189.4	195.9	−6.5
total	−819.9	−795.8	−24.1
Watson–Crick base pairs			−3.4
base stacking			−1.7
phosphate interactions			−6.1

Minimization of GC10

We note that GC10 taken from optimized structures of its complexes with neothramycin (GC10_X1) and anthramycin minimized to lower energy than the one taken from Arnott' B-DNA model (GC10_Xa). This is presumably because the latter optimized to a poorer local minimum. The differences between GC10_X1 and GC10_Xa are discussed as an example of this observation (Table VII).

Electrostatic forces account for most of the −24.1 kcal/mol total energy difference between the two structures. Bond angle and dihedral and van der Waals forces make moderate contributions, with angle strain favoring GC10_Xa. Also included in Table VII are the differences in energies for Watson–Crick base pairs, base stacking, and interactions of phosphate groups with attached sugars, neighboring bases, and neighboring phosphates. These differences were obtained by summing the energies for interactions by residue over each entire polynucleotide (data not shown) and then subtracting GC10_Xa from GC10_X1. They account for about half of the overall energy difference. There also was a significant difference in the number of C2′ endo sugar puckers in the two minimized decanucleotides. Thus, GC10_X1 had 14 C2′ endo, 5 C1′ exo, and 1 O1′ endo puckers, whereas GC10_Xa had 10 each of C2′ endo and C1′ exo puckers.

We note that the total energies of the energy-refined decanucleotides starting from the geometry in the anthramycin- and neothramycin–DNA complexes differ by more than 2 kcal/mol. This is because the two drugs are of different sizes and shapes and bind to the oligonucleotides to different extents, inducing slightly different conformational changes in the two sets of polynucleotides, resulting in two sets of local minima which are structurally closely related.

Comparing the complexes of neothramycin and anthramycin with the decanucleotides, we note that the configuration at C-11 is respectively *S* and *R* in the energetically most favored models. An exception is noted for NEO–G10C10, where the model with *S* configuration is energetically close to that with the *R* configuration. Both drugs show preferential binding to G10C10 over GC10, a fact reflecting consistency with experimental data for anthramycin–DNA complexes, but not for neothramycin–DNA complexes. The net binding energies of anthramycin to various A- and T-containing sequences of DNA are very close, while they differ significantly for neothramycin. The

drug distortion energy is generally higher for anthramycin (by 3 to 5 kcal/mol) compared to that of neothramycin.

Conclusions

Molecular mechanics simulations on anthramycin- and neothramycin-DNA complexes using an all atom force field have been presented and the simulated models are found to be qualitatively similar to the corresponding united atom models. The drugs are snugly packed in the minor groove of the oligonucleotides and the stabilization of the drug-DNA complexes is through good packing and electrostatic interactions. The lack of any major distortion in the DNA component of the complexes is consistent with NMR studies. In contrast to earlier studies on complexes between PBDs and pentanucleotides,[20] no transitions are observed in the decanucleotides from the B form of DNA. As in the united atom simulations, there is no marked preference or lack of it for the two drugs binding to A- and T-containing oligonucleotides.

The calculations are qualitatively consistent with the experimentally observed preference of anthramycin binding to puGpu sequences compared to pyGpy sequences. However, for neothramycin, the calculated binding preference to puGpu sequences is in apparent contradiction to the experimentally observed binding preference of the drug to poly(dG·dC)·poly(dG·dC). This could be due to the lack of explicit representation of solvent and counterion environment as well as lack of inclusion of molecular dynamic effects. It must be pointed out that the electrostatic interactions are treated in a very simplistic manner in the force field employed and this could lead to overemphasis of stabilizing interactions between the phosphates and complementary groups on the drugs, particularly in the anthramycin-DNA complexes where the amide side chain interacts with the ionic phosphates.

Experimental Section

The starting structures of the complexes between the DNA decamers on one hand and neothramycin and anthramycin on the other were obtained as described in our earlier studies on drug-DNA complexes.[11,19,26-28] The model-built structures were energy minimized as earlier with AMBER(UCSF)[21] and all atom force field parameters presented by Weiner et al. (1986).[22] The starting structure for the DNA decamers was B-DNA[29] and those for the drug molecules were based on the X-ray crystal data of anthramycin.[10] The decamers in the complexes were d-(GCGCGCGCGC)$_2$, d(G$_{10}$)·d(C$_{10}$), d(GCGCGAGCGC)·d-(GCGCTCGCGC), d(GCGCGTGCGC)·(GCGCACGCGC), d-(G$_5$AG$_4$)·d(C$_4$TC$_5$), and d(G$_5$TG$_4$)·d(C$_4$AC$_5$) and are abbreviated here as GC10, G10C10, GC10A6, GC10T6, G10C10A6, and G10C10T6, respectively. The complexes with anthramycin and neothramycin have been designated with the prefixes ANT and NEO, respectively. In the case of anthramycin-DNA complexes, only the 3′-orientation of the drug was considered while both 3′- and 5′-directions were modeled for neothramycin.

As earlier, we have carried out component analyses of energies of interactions in order to estimate the relative energetic stabilities of various complexes. For comparing the relative binding interactions for a drug with different polynucleotides, the net binding energies are used. They are calculated by subtracting the helix distortion and drug distortion energies from the total drug-DNA interaction energy. These distortion energies reflect induced fits that permit stronger intermolecular interactions. Drug and helix distortion energies are obtained by subtracting the energies of the minimized isolated drug or helix from their energies that occur in the complexes. In addition, we have evaluated the energy of interaction between the drugs and nucleotide residues (sugars, phosphates, and bases) spatially closely located to them. These are schematically illustrated in Figure 2.

The present investigation differs somewhat from our previous investigations in the way in which we have evaluated the helix distortion energies of the oligonucleotides in the complexes. Earlier, the isolated helix energies were calculated by starting from Arnott's B-DNA geometry and refining the energy with AMBER. However, for reasons stated earlier, in this study we have followed a strategy of starting with the minimized complex, removing the drug, replacing the hydrogen on the guanine (GUA5) where alkylation occurred, and reminimizing the structure. Although this method does not necessarily give the global minimum, the energy of the isolated DNA can be substantially lower than that obtained by starting from Arnott's B-DNA geometry.

Acknowledgment. We thank the Drug Design Group of Searle Research and Development for the computational facilities which were used in the calculations on anthramycin-DNA complexes. One of us (W.R.) thanks Professor Peter Kollman, University of California, San Francisco, for providing a copy of the program AMBER(UCSF) (version 3.0).

Supplementary Material Available: Tables listing base-stacking interactions and energies (Table IV), backbone dihedrals and sugar-base torsions (Table V), and phase angles (Table VI) for complexes and Figures 11–14 showing stereo pairs of energy-minimized complexes (7 pages). Ordering information is given on any current masthead page.

(26) Rao, S. N.; Singh, U. C.; Kollman, P. A. *J. Am. Chem. Soc.* **1986**, *108*, 2058.
(27) Remers, W. A.; Rao, S. N.; Singh, U. C.; Kollman, P. A. *J. Med. Chem.* **1986**, *29*, 1256.
(28) Remers, W. A.; Rao, S. N.; Wunz, T. P.; Kollman, P. A. *J. Med. Chem.* **1988**, *31*, 1612.
(29) Arnott, S.; Campbell-Smith, P.; Chandrasekharan, R. In *CRC Handbook of Biochemistry*; Fasman, G. D., Ed.; CRC: Cleveland, OH, 1976; Vol. 2, pp 411–422.